Annals of Biomedical Engineering, Vol. 33, No. 10, September 2005 (© 2005) pp. 1387–1404
DOI: 10.1007/s10439-005-4698-y

3-D Nanomechanics of an Erythrocyte Junctional Complex in Equibiaxial and Anisotropic Deformations

CARLOS VERA,[1] ROBERT SKELTON,[2] FREDERIC BOSSENS,[2] and LANPING AMY SUNG[1]

[1]Department of Bioengineering, and [2]Department of Mechanical and Aerospace Engineering, Jacobs School of Engineering, University of California, San Diego, La Jolla, California 92093

(Received 18 July 2003; accepted 24 March 2005)

Abstract—The erythrocyte membrane skeleton deforms constantly in circulation, but the mechanics of a junctional complex (JC) in the network is poorly understood. We previously proposed a 3-D mechanical model for a JC (Sung, L. A., and C. Vera. Protofilament and hexagon: A three-dimensional mechanical model for the junctional complex in the erythrocyte membrane skeleton. *Ann Biomed Eng* 31:1314–1326, 2003) and now developed a mathematical model to compute its equilibrium by dynamic relaxation. We simulated deformations of a single unit in the network to predict the tension of 6 $\alpha\beta$ spectrin (Sp) (top, middle, and bottom pairs), and the attitude of the actin protofilament [pitch (θ), yaw (ϕ) and roll (ψ) angles]. In equibiaxial deformation, 6 Sp would not begin their first round of "single domain unfolding in cluster" until the extension ratio (λ) reach $\sim$3.6, beyond the maximal sustainable λ of $\sim$2.67. Before Sp unfolds, the protofilament would gradually raise its pointed end away from the membrane, while ϕ and ψ remain almost unchanged. In anisotropic deformation, protofilaments would remain tangent but swing and roll drastically at least once between $\lambda_i = 1.0$ and $\sim$2.8, in a deformation angle- and λ_i-dependent fashion. This newly predicted nanomechanics in response to deformations may reveal functional roles previous unseen for a JC, and molecules associated with it, during erythrocyte circulation.

Keywords—Actin, Nanomechanics, Deformation, Protofilament, Spectrin.

INTRODUCTION

Circulating erythrocytes have remarkable deformability essential for their passing through small capillaries in tissues and narrow sinusoid slits in the spleen. The architecture of the membrane skeleton allows erythrocytes to travel in deformed states and recover to their biconcave shape in low-stress states. The network also provides restrained viscoelasticity during deformations to ensure the integrity of the lipid bilayer. During the lifetime of erythrocytes, small and neutral molecules like oxygen diffuse through the lipid bilayer, and charged ions or larger molecules are transported or diffused through various membrane-associated transporters or channel proteins, respectively. However, very little is known about the nanomechanics of the membrane skeletal network and its components in each basic unit and the functional role of nanomechanics during erythrocyte membrane deformation.

The human erythrocyte membrane skeletal network consists of small "spoked" hexagons (basic repeating units) formed by a junctional complex (JC) with 6 $\alpha\beta$ spectrin dimers (Sp) radiating from a central short actin protofilament and up to six associated suspension complexes (SC).[38] Each short actin protofilament of approximately 37 nm, may be capped by erythrocyte tropomodulin (E-Tmod) at the pointed end, and bracketed by 2 tropomyosin (TM) molecules of isoform 5 or 5b of about 33–35 nm. The E-Tmod/TM/actin complex may function as a mechanical axis for three (top, middle, and bottom) well-defined Sp pairs.[38]

A SC contains band 3 protein which is a transmembrane anion exchanger (AE1), protein 4.2 which is a pseudo-transglutaminase associated tightly with the lipid bilayer, and ankyrin which is a cyclin-homolog bearing a β-spectrin-binding site at its 15th domain. Such organization allows SC to function as the primary site for pinning the actin-Sp based membrane skeleton network to the lipid bilayer.[3] Another major transmembrane protein, glycophorin C, via the association with protein 4.1R and the JC, provides a secondary site.[30] There are other proteins associated with JC or SC, which are not included in our current model. For a detailed review of the spectrin and ankryin-based networks see Bennett *et al.*[2]

Sp has an elongated structure and, like many proteins exposed to mechanical tension, contains multiple individually folded domains.[7] Unfolding and refolding of domains could be a mechanism by which tension is maintained in these molecules during cell deformation.[26] In erythrocytes, α and β spectrin have 21 and 17 domains, respectively, arranged in antiparallel fashion.[19] Each of these homologous domains

Address correspondence to Professor Lanping Amy Sung, PhD, Department of Bioengineering, and Center for Molecular Genetics, Mail Code 0412, University of California, San Diego, 9500 Gilman Drive, La Jolla, California 92093-0412. Electronic mail: amysung@bioeng.ucsd.edu

has about 106 amino acids and is made of three antiparallel α helices, folded into a left coiled-coil[36] with each domain interconnected by helical linkers. Force spectroscopy involving single domain unfolding of spectrin extracted from human erythrocytes has been established using atomic force microscopy (AFM)[31] and the saw-tooth force–extension curve of spectrin has been modeled using the worm-like chain (WLC) paradigm.[5,31] However, the tension in each of the 6 Sp (within a basic unit) in response to mechanical deformation, and whether any of the Sp unfolds during physiological deformation of erythrocytes remain unknown. It is also not clear whether the folding and unfolding of Sp and/or other factors may govern the orientation of protofilaments in the natural and deformed states of erythrocytes.

In an attempt to answer the above questions, we developed a mathematical model for a JC to simulate the tension of Sp and the attitude of a protofilaments within a basic unit in response to defined deformations (Appendix). This model is based mainly on (1) the proposed 3-D model for a JC,[38] in which each pair of Sp (i.e., Sp_1/Sp_2, Sp_3/Sp_4, or Sp_5/Sp_6) are arranged in a back-to-back fashion, and three pairs of Sp spiral down the protofilament from the pointed end to the barbed end, (2) the force–extension curve of spectrin experimentally obtained by AFM,[31] modeled using the WLC paradigm[5] that incorporated the unique feature of modular elongation,[35] and (3) the published results for the ultrastructural organization of the membrane skeletal network by transmission electron microscopy (TEM).[6,25,33] The simulation was achieved by solving the 6 degree-of-freedom model, and the dynamic relaxation method was used to find the final steady state values. Within a basic unit, a change of tension in any Sp would alter the attitude of the protofilament [described by pitch (θ), yaw (ϕ), and roll (ψ) angles], and any movement of the protofilament as a rigid body, in turn, would alter the tension in every Sp. This process would continue until eventually a new equilibrium state is reached. The outcome of this model is a prediction for the final orientation of a JC, and the length and tension in each of the six associated Sp, within one basic unit undergoing either equibiaxial deformation or constant area anisotropic deformation.

The micropipette aspiration technique, which generates well-defined modes of erythrocyte deformation, has been extensively used since early 1970s.[8,13,37] Membrane aspiration into the micropipette produces an equibiaxial deformation at the hemispherical cap, and a large anisotropic constant area deformation at the cylindrical projection. More recently, fluorescence imaged microdeformation suggests that a sustainable network extension (λ) in dilation at the hemispherical cap was approximately $\sqrt{7}$ (or $\sim$2.67) relative to the natural state of the membrane network.[12] Fluorescence-patterned photobleaching also show that the protein network is capable of sustaining large anisotropic constant area strains in the area of cylindrical projection with local extensions as great as $\sim$2–3 in the axial direction (λ_1), simultaneously accompanied by contractions of at least 0.4 in the circumferential direction (λ_2) in the cylindrical projection.[11,24] The sustainability of the network [i.e., the network held large chemical gradients over a long period of time ($\sim$30 min)] suggested that the structure of the network remained intact under these stressed conditions.

While tensions of Sp inside erythrocytes have not been measured, there are testable predictions for two of the three angles that we used to describe the attitude of a protofilament (i.e., θ and ϕ) in erythrocytes under well-defined deformations measured by fluorescent polarization microscopy (FPM).[28,29] It was found that greater than 60% of the protofilaments measured by FPM in both the natural state ($\lambda = 1$) and osmotically sphered erythrocyte ghosts[29] ($\lambda \sim 1.03$)[15] had a pitch angle $\leq 22^\circ$, at least within the 15° to 20° resolution of current methods. Therefore, these protofilaments were more tangent than normal to the lipid bilayer. Furthermore, imaging of micropipette-deformed erythrocyte ghosts showed that protofilaments had the same membrane-tangent orientation at the hemispherical cap and over the length of the network projection pulled into the micropipette.[28] As to the yaw angle, protofilaments were found to continue to exhibit near-random azimuthal orientation (corresponding to the yaw angle in our model) along the length of the network projection in very large micropipette-deformations.[28] Our model predictions are in agreement with experimental FPM data about pitch and yaw angles of the protofilament in these deformation states.

Traditional methods of modeling the erythrocyte membrane have focused on the macroscopic scale (continuum models)[14,39]. A finite element network model was developed based on the microstructure of the erythrocyte membrane skeleton, but the JC was treated only as a mechanical node.[17,18] Coarse-grained molecular models have also been presented in Monte Carlo simulations of a whole erythrocyte in micropipette aspiration,[10,28] but the JC was modeled as a 2-D three-polymer chain. None of the above models predict the 3-D attitude of the protofilament and the tension in each Sp with a feature of modular elongation in response to membrane skeletal deformations.

For the first time, we are able to predict the 3-D nanomechanics of a JC in a single unit of the erythrocyte membrane skeleton in different deformation states. In this paper, we reported two physiologically significant deformation states (equibiaxial deformation and constant area anisotropic deformation). Our model predicted that (1) in equibiaxial deformation, 6 Sp would not begin their first round of "single domain unfolding in cluster" until $\lambda \sim 3.6$, beyond the maximal sustainable λ of $\sim$2.67; (2) before any Sp unfolding, the protofilament would gradually raise its pointed end away from the membrane, while ϕ and ψ remain unchanged; and (3) in anisotropic deformation, protofilaments would remain tangent but swing and roll drastically at least

once between $\lambda_i = 1.0$ and ~2.8, in a deformation angle- and λ_i-dependent fashion. This newly predicted nanomechanics in response to deformations may pave the way to uncover the potential roles for the nanomechanics of a JC previously unseen during erythrocyte circulation.

METHODS

Mathematical Model

A mesoscale mathematical model was developed to simulate the dynamics and the final steady state of a JC (Appendix). We used the dynamic relaxation method to find the equilibrium, which allows predictions of the dynamics and the final steady state of a JC responding to various mechanical deformations. In this method, we give the protofilament an arbitrary initial position (in general out of the equilibrium), and compute its motion over time, which eventually stabilizes (provide some damping is present in the model) in the static configuration we seek to calculate.

Natural State

The natural state is defined as the condition of the membrane skeletal network in which the erythrocyte is not subjected to any external force. At this state, the deformation ratio (λ) = 1, and the larger hexagon (consists of 6 + 1 small edge-free hexagons) has 75 nm in length for each side.[6,25,33] At the first attempt, we assumed that each SC is ~30 nm away from the center of the small edge-free regular hexagon [see SC_1 or SC_2 in Fig. 1(a)]. The positions of 6 Sp attachment points on a protofilament (top view) and the coordinates of the SC (h_i^r) in the lipid bilayer are now defined [Fig. A2(a) and Table A1].

Equibiaxial Deformation

Simulations were performed with equal deformation ratios in the x and y directions ($\lambda_1 = \lambda_2$). This includes the

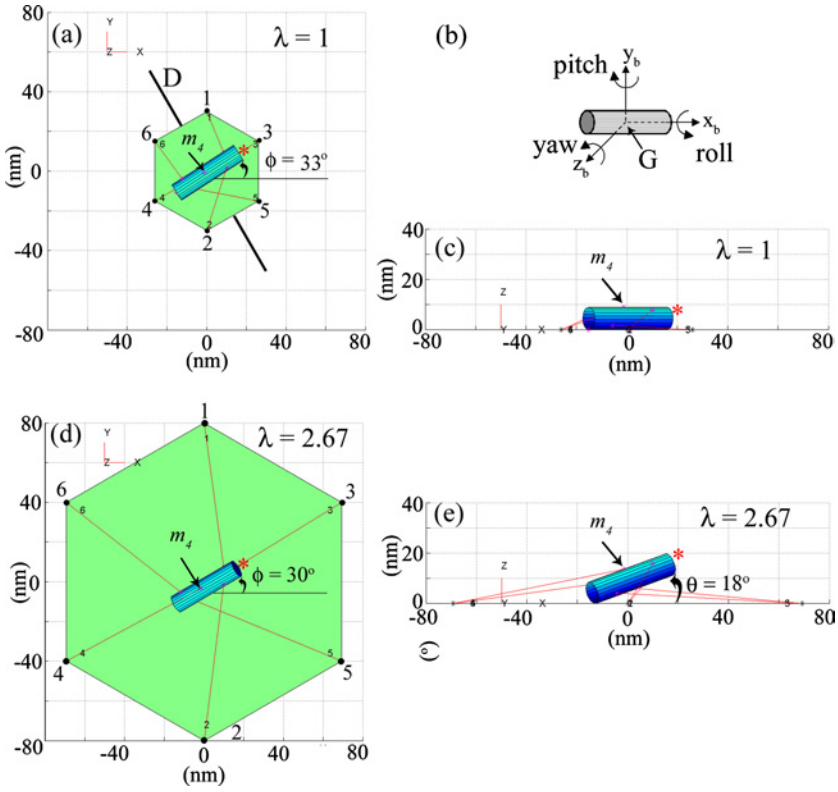

FIGURE 1. The final equilibrium conditions of a protofilament at the natural state ($\lambda = 1$) and the equibiaxial deformation at $\lambda = 2.67$. The upper panels are for the natural state. (a), (c) are top and side views, respectively; (b) shows the orientations for the roll (ψ), pitch (θ), and yaw (ϕ) angles in the $\{x_b, y_b, z_b\}$ reference frame. The top view shows a protofilament connected through three pairs of Sp (i.e., Sp_1/Sp_2, Sp_3/Sp_4, and Sp_5/Sp_6) to six corresponding SC. The order of SC, numbered next to the hexagon, is according to the proposed sequence of the Sp attached to the protofilament. The attachment sites of these 6 Sp are based on our mechanical model,[38] and numbered from the pointed end to the barbed end. Lower panels are for the equibiaxial deformation at $\lambda = 2.67$; (d) and (e) are the top and side views, respectively. Line D in (a) divides the hexagon into two halves: one that has SC or Sp in odd numbers (i.e., 1, 3, and 5) and the other one in even numbers (i.e., 2, 4, and 6). The pointed end of the protofilament capped by E-Tmod is marked with an asterisk. Note that the line between each Sp-binding site on the protofilament (m_i) and corresponding SC_i, represents the distance (Sp "effective length") and not the Sp contour length.

maximal sustainable equibiaxial deformation condition of $\lambda_1 = \lambda_2 = 2.67$. The distances are approximately 200 nm between the JC, 80 nm between the JC and the SC, and 40 nm between neighboring SC on the spectrin tetramer. In this case, the final coordinates of SC in lipid bilayer (h_i^e) were defined to match this geometry (Table A1). For the wider range analysis reported here, deformation ratios were increased from $\lambda = 1$ to 8 with a step of 0.33. Smaller increments were used in several critical regions where the protofilament attitude or the Sp tension changes dramatically, in respect to Sp unfolding. From here on λ refers to the equibiaxial deformation ratio.

Anisotropic Deformation

Simulations of anisotropic deformation were performed assuming constant area deformation ($\lambda_1\lambda_2 = 1$). Anisotropic strains were in the range of λ_1 from 1 to 8, with a step of 0.33, and the deformation angle (τ) varied from 0° to 180°, with a step of 15°. At several critical regions, where the protofilament attitude or the tension of Sp changes dramatically with increasing deformation ratios, smaller increments were used. From here on λ_i refers to the anisotropic deformation ratio. The principal assumption in anisotropic deformation simulations was a constant area network during deformation. It is know that the isolated membrane skeleton is expandable (and compressible) and can be deformed with limitless possibilities. However, the network is attached to the lipid bilayer which has physical constrains of having a constant area and incompressibility. Without constrain of constant area, i.e., allowing the membrane skeletal network to overextend instantaneously, the lipid bilayer would rupture and cause hemolysis of erythrocytes. Therefore, constraining the deformation to a constant area in anisotropic deformations is based on the normal physiology of erythrocyte membranes. In modeling a local dilation, i.e., an equibiaxial deformation, however, constant area is not maintained, and the inflow of the lipid bilayer is considered as a mechanism to prevent hemolysis under physiological condition.

RESULTS AND DISCUSSION

The precise attitude of the protofilament and the tension in each Sp in a JC of the erythrocyte membrane skeleton may be physiologically and pathologically important. A dynamic model that includes the entire erythrocyte network (~33,000 JC) would be very interesting but extremely difficult to implement at present. In this study, we present a mesoscale mathematical model to predict the 3-D mechanics of a JC in a single unit, without the influence of adjacent units. This model is ultimately aimed at illustrating the mechanical events of individual components (molecules and/or molecular complexes) in the network during erythrocyte deformation in circulation, and their potential roles in health and disease. This may be accomplished by (1) predicting the attitude of protofilaments, which is a nanostructure in a JC, and the tension in each of the 6 Sp, which is in the order of pN, in natural and various deformed states of erythrocytes; and (2) finding the meaning and consequences of these predicted outcomes.

Despite its simplicity, this mathematical model provides valuable information previously unseen. Without quantitative descriptions, it would be impossible to imagine the potential contributions of these structural elements in nanometer scale and forces at pN level in various physiological and pathological conditions. With this goal in mind, we may simulate as many deformation states as possible, including uniaxial deformation at constant orthogonal length, and the deformation in which the orthogonal force resultant is zero, as well as extend the model to simulate networks consisting of larger numbers of basic units. The choices of deformation modes simulated in this report, namely, the equibiaxial and constant area anisotropic deformations, have several advantages in terms of experimental validations and modeling history, since one of the best methods to characterize the mechanics of the erythrocyte membrane since the early 1970s has been to induce and model well-defined deformations by the technique of micropipette aspiration.[8,13,37] Below we outline the nanomechanics of a JC in a single unit of the erythrocyte membrane skeletal network, based on the model predictions in equibiaxial and anisotropic deformations.

Protofilaments in "Natural State" and Hypotonically Sphered Erythrocyte Ghosts

One actin protofilament associated with 6 Sp and connected potentially to 6 SC is defined as the basic repeating unit[38] for the erythrocyte membrane skeleton. The final attitude of a protofilament associated with 6 Sp in the natural state of erythrocytes (see Methods section) is graphically represented in Fig. 1. The top view [Fig. 1(a)] shows the protofilament positioned in the basic unit (a small edge-free hexagon) with a yaw angle (ϕ) of 33°, with its pointed end (marked with an asterisk) pointing toward SC_3 and the barbed end toward SC_4. In addition, the attachment site of Sp_4 (the number 4 Sp from the pointed end) on the protofilament (marked as m_4) is found to face upward with a roll angle (ψ) = 58°. The side view [Fig. 1(c)] shows that the pitch angle (θ) = 0° (tangent to the membrane), implying that the protofilament would be in contact along its full length with the cytoplasmic side of the lipid bilayer.

In the natural state, the values of ϕ and ψ would be relatively insensitive to the values of the vertical stiffness (K_m) [See Appendix, under Contact between Protofilament and Lipid Bilayer (k_m)], since they would be relatively constant when $0 \leq K_m \leq 200$ pN/nm [Fig. 2(a)]. The values of θ would converge to and remain 0° when $K_m \geq 5$ pN/nm. FPM experiments have revealed that protofilaments in the "natural state" ($\lambda = 1$) and hypotonically

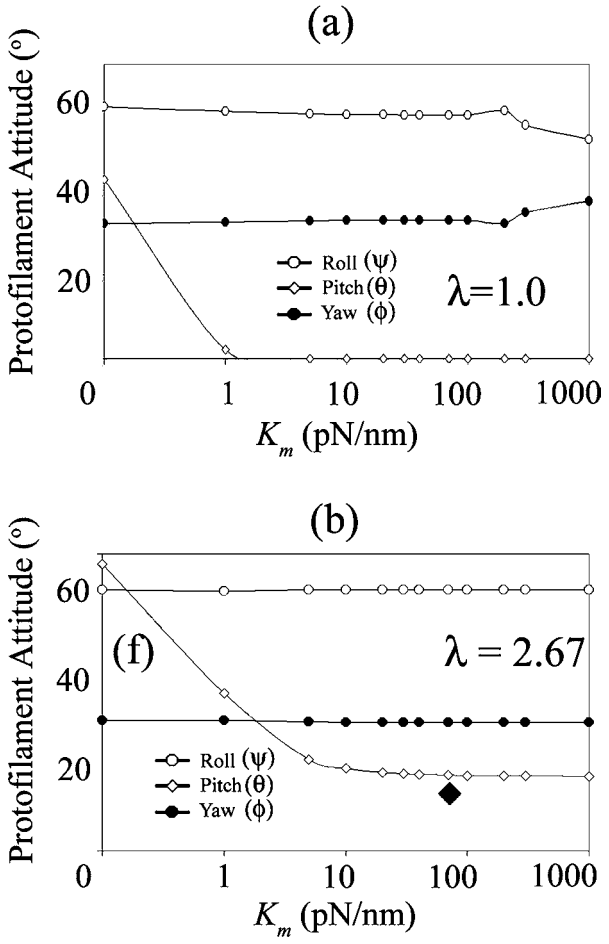

FIGURE 2. The attitude of protofilament in a single unit of the erythrocyte membrane skeleton vs. K_m. The orientation of protofilaments is expressed by the angles: roll (ψ), pitch (θ), and yaw (ϕ) at the (a) natural state ($\lambda = 1$), and (b) maximal sustainable (equibiaxial) deformation ($\lambda = 2.67$) as a function of K_m values.

sphered erythrocyte ghosts ($\lambda \sim 1.03$) were relatively more tangent than normal in orientation to the membrane, with more than 60% of the Gaussian distribution of protofilaments having angles between 0° and 22° from the plane of the lipid bilayer.[28,29] Since the resolution of the FPM was within 15° to 20°,[28] our predicted $\theta \leq 22°$ at $\lambda = 1$ and 1.03 when $K_m \geq 0.2$ pN/nm would not be inconsistent with the experimental data.[28,29] In hypotonically sphered erythrocyte ghosts ($\lambda = \sim 1.03$), our model does not consider the conformational changes of Sp induced by hypotonicity per se.[26]

Protofilaments at Maximal "Sustainable" Equibiaxial Deformation

The attitude of a protofilament at the maximal "sustainable" deformation ($\lambda = 2.67$) in a local deformation of the membrane skeleton (see Methods section) is also graphically represented in Fig. 1. The top view [Fig. 1(d)] shows the protofilament would remain in the same direction, and the Sp_4 attachment site still faces upward on the protofilament. The side view [Fig. 1(e)], however, shows that θ would be ~18°. This value would be in agreement with the experimental finding that protofilaments remained more tangent than normal to the membrane in the hemispherical cap, which was produced by micropipette aspiration of erythrocytes and undergoing an equibiaxial deformation.[28]

Figure 2(b) again shows that the values of ϕ and ψ would be constant regardless of the value of K_m, and that the value of θ would converge to 18° when $K_m \geq 10$ pN/nm. Under the extreme condition with $K_m = 0$, the model would predict an almost upright protofilament ($\theta = 69°$) that (together with Sp) may intrude or displace the lipid bilayer by 19 nm. Because the actual value of K_m is not available, a value of 87.5 pN/nm for K_m [marked by ♦ in Fig. 2(b)] has been used in all later simulations due to the robustness of protofilament orientation with $K_m \geq 10$ pN/nm.

Pointed End of a Protofilament

The values of ϕ, ψ, and θ for a protofilament in the range of $\lambda = 1$ to 8 are predicted and presented in Fig. 3(a). Despite the fact that this model does not assign different properties to the two ends of the protofilament, the pointed end would have a tendency to move upright or away from the lipid bilayer (while the barbed end remains associated with the cytoplasmic side of the lipid bilayer), when tension of 6 Sp increases with increasing λ [Fig. 1(e)]. The connectivity of 6 Sp to the protofilament[38], therefore, may be responsible for this mechanical behavior. This is interesting since in the leading edge of motile cells, or in several other cell types (e.g., inner ear cells), actin filaments have been found to have a preferred orientation with the barbed end positioned toward the membrane. It is also interesting to point out that no mathematical model for the pitch angle simulations has ever been reported. Our model, therefore, represents the first mathematical simulations for the pitch angle measurement.

First Unfolding of a Sp Domain

It is noted that with increasing values of λ, ϕ, and ψ would remain relatively constant, but θ would increase linearly from 0° to 30° until the first unfolding of a Sp domain [left arrow in Fig. 3(a–c)] occurs. When a JC is subjected to an equibiaxial deformation, the first unfolding of a Sp domain would occur in Sp_5 at λ of ~ 3.6. Each sudden unfolding of a domain in a Sp would lead to a sharp change in θ, ϕ, and ψ. While ϕ and ψ would tend to come back to their original values, there is a tendency for θ to continue higher with increasing λ.

Sp has been considered as the principal determinant of erythrocyte membrane network elasticity. Unfolding and refolding (modular elongation)[26] of Sp domains has been

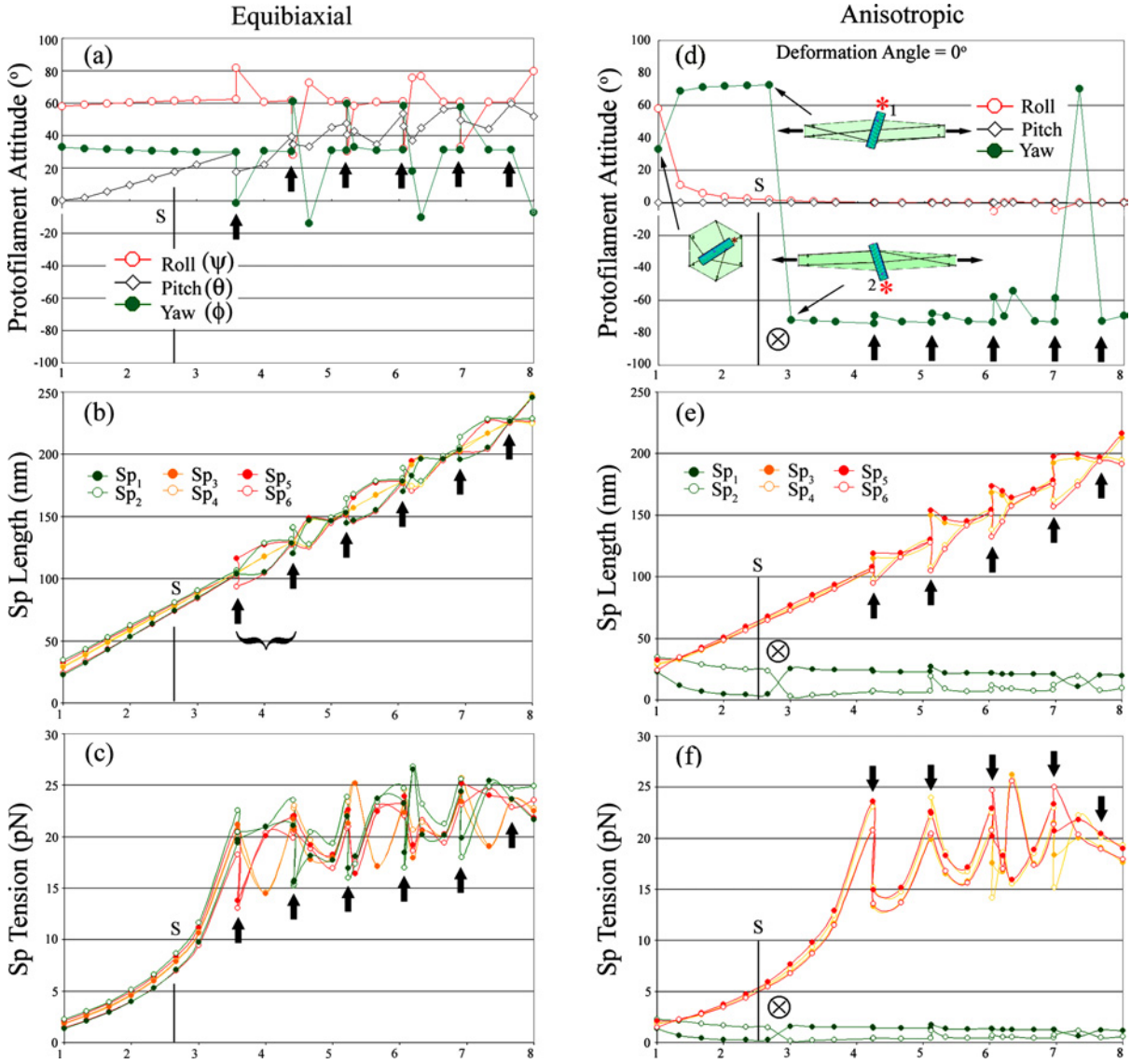

FIGURE 3. The attitude of a protofilament and the length and tension of 3 pairs of Sp at equibiaxial and anisotropic deformations. The left panels are for equibiaxial deformations where $\lambda_1 = \lambda_2 = 1$ to 8. (a) Shows the attitude of the protofilament; (b) and (c), the length and tension of each of the 6 Sp, respectively. The right panels are for constant area anisotropic deformations where $\lambda_1 = \lambda_2^{-1} = 1$ to 8 with a deformation angle (τ) = 0°. (d) Shows the attitude of the protofilament; (e) and (f), the length and tension of Sp, respectively. Three insets in (d) are the top views of a repeating unit at $\lambda_1 = 1$, 2.67, and 3.0, respectively. The pointed end of the protofilament is indicated by an asterisk. Each pair of Sp are color-coded; Odd, solid symbols; Even, open symbols. Six arrows in (a–c) and five in (d–f) indicate the beginning of "single Sp domain unfolding in cluster", after each Sp reaches 30 pN in tension. ⊗ indicates λ_1, between 2.67 and 3, where ϕ and ψ change suddenly, dramatically, and simultaneously, along with the transition of Sp_1 and Sp_2 from a crossing to an open configuration. The S lines stand for maximal sustainable deformation values (λ of ~2.67 for equibiaxial deformation and λ_i of ~2.5 for anisotropic deformation). The Sp length refers to the "effective length" (see Methods section).

proposed as a mechanism by which tension is maintained.[5] Our simulations, however, show that the first unfolding of a Sp domain would occur at a deformation ratio ($\lambda \sim 3.6$) beyond the maximal sustainable deformation ($\lambda = 2.67$).[12] This finding suggests that the nonlinear elasticity of Sp (before the first unfolding) may be sufficient to maintain the tension within the sustainable ranges of erythrocyte deformation *in vivo*, and that the modular elongation of Sp may serve as an additional mechanism by which the integrity of the membrane network may be maintained in larger deformations. This result deserves additional analysis to elucidate the contribution of Sp unfolding to erythrocyte deformation in physiological and pathological conditions.

"Single Sp Domain Unfolding in Cluster"

This model predicts that the length of Sp would increase linearly in response to an equibiaxial deformation until λ reaches ~3.6. At this deformation ratio, Sp_5 would reach

112 nm and unfold one domain for the first time (see force spectroscopy curve of Sp modeled as a WLC in Fig. A3). This unfolding would allow an increase of ~31 nm in length and reduction in tension in Sp_5. In response to this unfolding, Sp_6 (the partner in the bottom pair of Sp) would reduce slightly in length and tension. Further analysis revealed that by the time $\lambda = 4$, each of Sp_2, Sp_3, and Sp_4 would have also unfolded one domain. By the time $\lambda = 4.4$, each of Sp_1 and Sp_6 would have also unfolded one domain. Each Sp is expected to unfold one domain when its length exceeds 112, 137, 162, 186, 211, and 234 nm sequentially [see arrows in Fig. 3(b)] each time when the tension reaches the threshold level of ~30 pN.[31] There are six rounds of "single Sp domain unfolding in cluster" before $\lambda = 8$. Figure 3(c) shows the increasing tension of each of the 6 Sp with increasing λ.

The adjustment of Sp length would occur progressively during deformation. After each domain unfolding, a new equilibrium would be reached among all 6 Sp. Only after each of the 6 Sp has unfolded one domain (not the complete unfolding of all domains), can the second round of unfolding begin. We, therefore, refer the process in each round from the beginning to the end of unfolding of one domain in each of the 6 Sp as "single Sp domain unfolding in cluster" [bracketed in Fig. 3(b)].

Yaw Angle as a Function of Deformation Angle

In anisotropic deformation, the deformation angle (τ) relative to the basic unit would affect the mechanics of the protofilament and Sp. Figure 4 shows the top view of a basic unit under a specific deformation condition when $\lambda_1 = \lambda_2^{-1} = 2$ so that the area remains constant. Six different τ angles, from 0° to 180° with an increment of 30° are shown. It is noted that the protofilament would orient close to being perpendicular to the deformation angle. Additional simulations show that ϕ (or the azimuthal angle) would be τ- and λ_i-dependent (Fig. 5). Here the attitude of the protofilament (including ϕ) vs. a wide range of λ_i (1–5) in 12 different τ (from 0° to 180° with an increment of 15°) is plotted. It is found that among the 12 conditions simulated, the absolute value of the angle between the longitudinal axis of the protofilament (ϕ) and the deformation angle (τ) is $76° \pm 6°$ (average $\pm$ SD). In other words, protofilaments under these conditions would not align with the deformation angle.

Previously, an affine deformation model predicted that lines representing protofilaments would have a propensity to align in the direction of the principal deformation.[28] Experimental data, however, showed that protofilaments continued to exhibit random azimuthal orientation in very large deformations.[28] A 2-D Monte Carlo simulation, in which each of the four short protofilaments was modeled as a stiff trimer of beads cross-linked by six longer flexible spectrin chains, showed that more than half the time, anisotropically stressing the network lead to a counter-rotation away from the average initial angle rather than an alignment in the spectrin-extended direction, supporting the nonaffine behavior of protofilaments during deformation. Our 3-D simulations agreed with the nonaffine behavior of protofilaments observed experimentally and predicted by the 2-D Monte Carlo simulation.[28]

Bifurcation of ϕ in Anisotropic Deformations

A dramatic change (a bifurcation of the equilibrium state) of ϕ may occur during anisotropic deformation, and the magnitude of the change may be τ dependent (Fig. 5). For example, when $\tau = 0°$ [Fig. 3(d)], the drastic change of ϕ (from 72° to −72°) would occur between $\lambda_i = 2.67$ and 3, which would be before the first Sp domain unfolding (indicated by a thick vertical arrow). Within this narrow range (indicated by $\otimes$) the point end of the protofilament would change from being near SC_1 to near SC_2 (see inserts). The change of ϕ would coincide with the change of Sp_1 and Sp_2 (the two more relaxed Sp) in their length [Fig. 3(e)] and tension [Fig. 3(f)]. The reasons for these bifurcations deserve more investigations, and are attributed to factors, which may include the 3-D geometrical arrangement of 3 Sp pairs on a protofilament[38] and the restricted freedom of SC within a basic unit. It would be interesting to see if a bifurcation of the equilibrium states also exists in multiunit simulations.

ϕ and ψ as a Function of Anisotropic Deformation Ratios

It is found that in all cases examined (Fig. 5), ϕ and ψ would undergo one or more dramatic and coordinated changes, and in some cases they would oscillate (e.g., $\tau = 90°$). Since random initial orientation (ϕ) of basic repeating units have been revealed by TEM in erythrocyte membrane skeleton, our model predicts that *any* minor anisotropic deformation would induce dramatic changes in both ϕ and ψ under physiological conditions (Fig. 5). In addition to the nonaffine behavior in anisotropic deformations, our 3-D model simulation further predicts that the yaw angle of a protofilament would not only depend on the deformation angle (τ), but also on the anisotropic deformation ratio (Figs. 4 and 5). This is a major difference from the 2-D Monte Carlo simulations, which used a coupling constant to describe the relationship between the azimuthal angles and the direction of maximal deformation.[28]

The dramatic changes in ϕ or ψ may create perturbations in the lipid bilayer and the network proteins. Such perturbation may result in increased diffusion of chemicals through the lipid bilayer, altered exchange or transport of molecules by membrane proteins, or potential damages to the membrane skeletal network. By the time λ_i reaches ~2.8, which is near the maximal sustainable anisotropic deformation ratio, all the protofilaments, regardless of their original ϕ

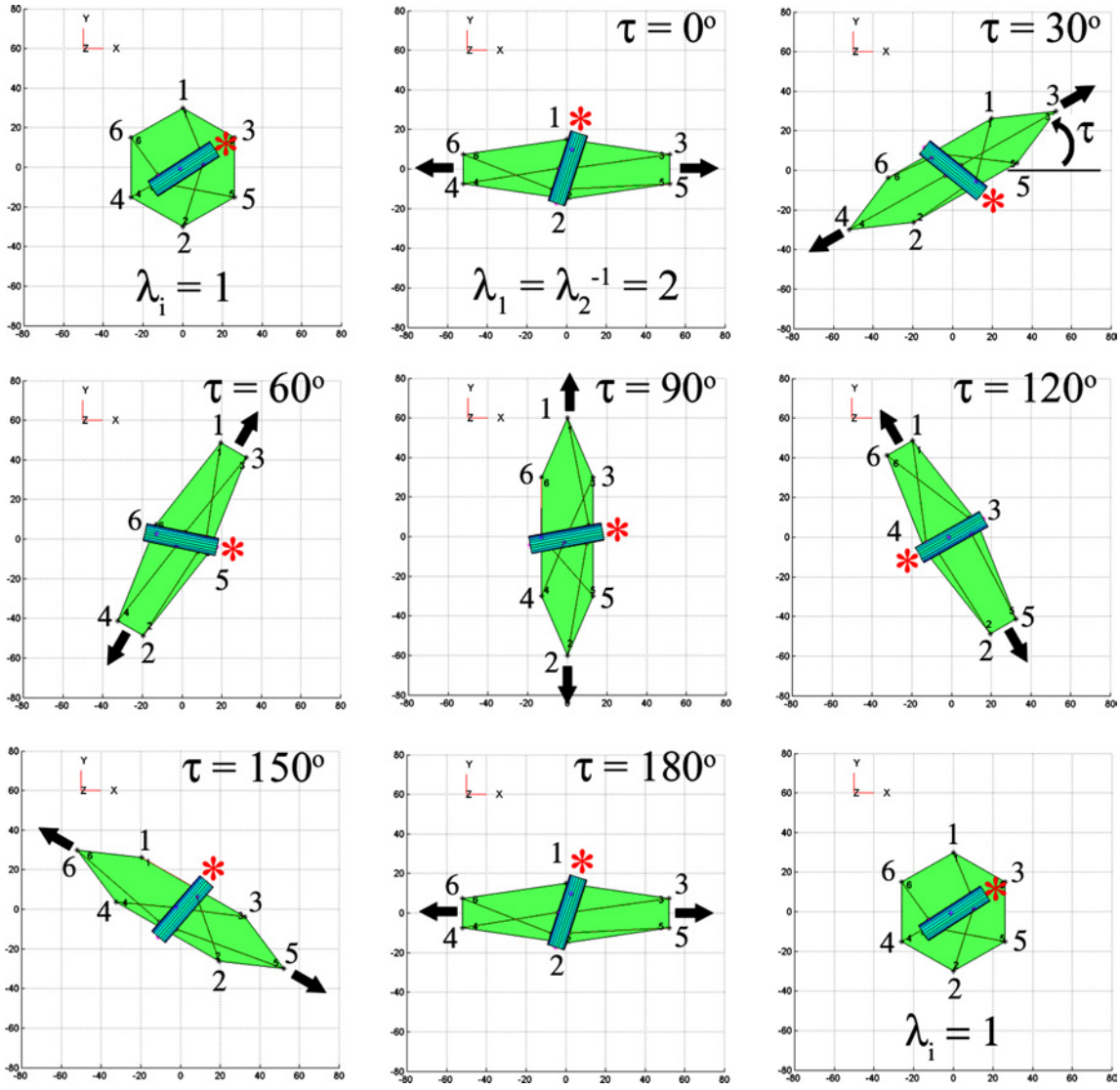

FIGURE 4. The top view of a JC in anisotropic deformation with different deformation angles (τ). The first and last panels are in natural state ($\lambda = 1$); other panels are in anisotropic deformation, $\lambda_1 = \lambda_2^{-1} = 2$, where τ (from 0° to 180°), indicated in the upper right corner, are the direction of the forces applied and presented by opposing arrows next to the deformed hexagon. The pointed end of the protofilament is marked with an asterisk. Numbers around the hexagon are that for corresponding SC and Sp. The basic repeating unit at $\lambda = 1$, or the natural state, is included (twice) for comparison. Note that $\tau = 0°$ and $\tau = 180°$ are topologically equivalent. The *x* and *y* axes are in nanometers.

and ψ angles, would have undergone the predicted dramatic changes. It would be interesting to see whether such changes or potential damages may be responsible for the unsustainable deformations of the erythrocyte membrane skeleton.

Independence of θ on Deformation Angle and Anisotropic Deformation Ratio

Figure 5 shows that in a constant area anisotropic deformation θ would remain $\sim 0°$ regardless of τ in a wide range of deformations. This is in agreement with experimental data obtained by FPM,[28] in which protofilaments maintained the tangent orientation over the erythrocyte projection (cylindrical portion) pulled into the micropipette, where the network is strongly deformed in axial extension and contracted in the circumferential direction.

In general, the rate of increase in Sp length is slower in the anisotropic deformation than that in the equibiaxial deformation [see slopes in Fig. 3(b) and (e)]. Therefore, it may require a larger deformation to unfold Sp domains in anisotropic deformation. In addition, in anisotropic deformation the degree of deformation among 6 Sp may be

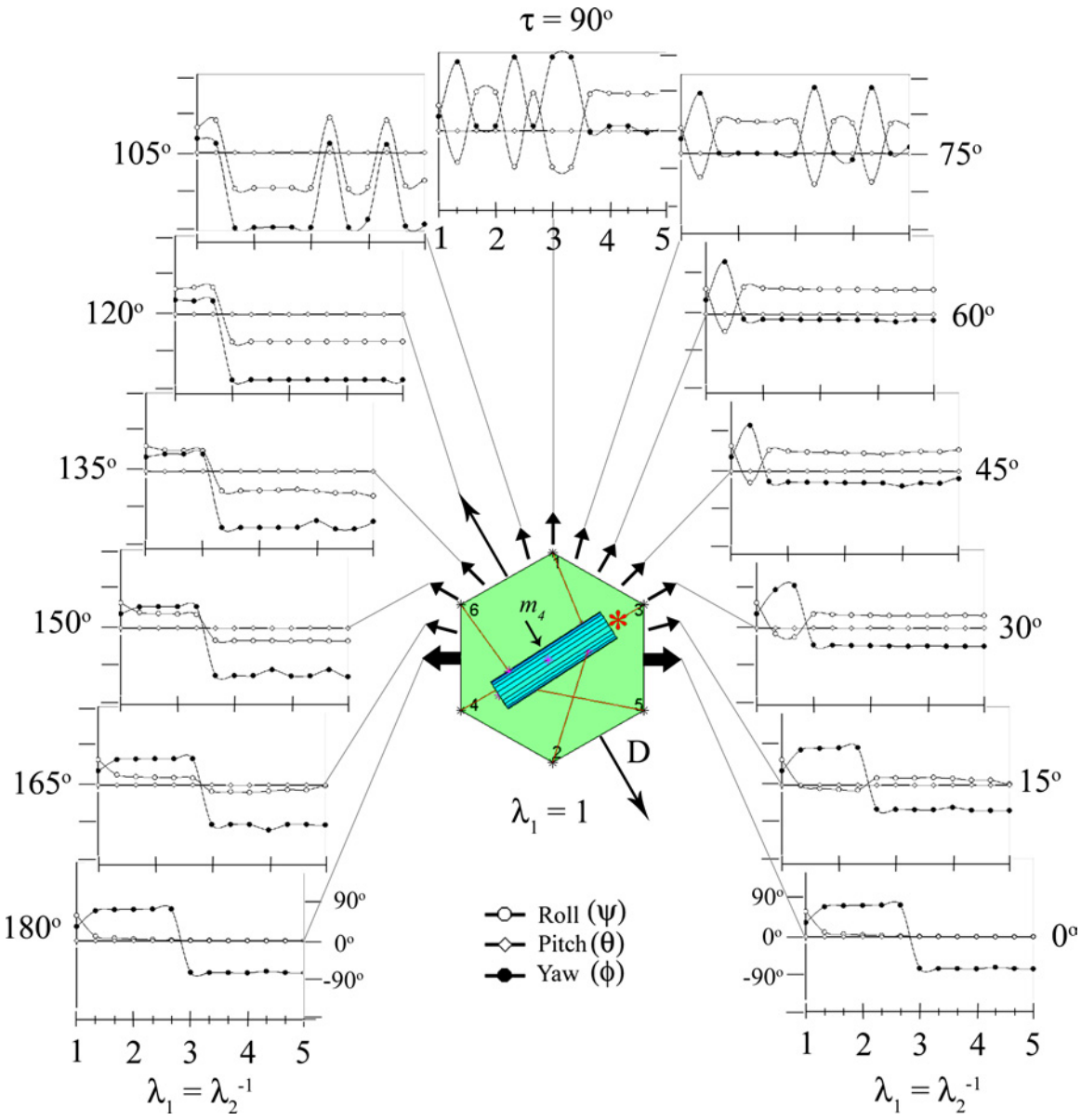

FIGURE 5. The effect of deformation angles (τ) on the attitude of the protofilament in anisotropic deformations where $\lambda_1 = \lambda_2^{-1} = 1$ to 5. The basic repeating unit as a small hexagon in the center, which contains a protofilament connected by three pairs of Sp to 6 SC, is shown at $\lambda_1 = 1$. Arrows indicate τ (from 0° to 180°) with an increment of 15°. The axis values are shown in panels of $\tau = 0°$ and 180°, which are identical. Two longer arrows in opposing directions, at $\tau = 120°$ and $-60°$, indicate the deformation along the D line that separates the small hexagon into two sides. The pointed end of protofilament capped by E-Tmod is indicated by an asterisk. View the trend of changes in ψ (close circle) and ϕ (open circle). Deformation angles (τ) are shown in the outer margin.

dramatically different [Fig. 3(e)], while in the equibiaxial deformation all 6 Sp behave more similarly [Fig. 3(b)].

Unfolding of Sp in Anisotropic Deformation

Figure 3(e) and (f) show the predicted effective length and tension of each of the 6 Sp vs. λ_i, when $\tau = 0$. The length and tension of the middle and bottom pairs are predicted to increase gradually until the first "single domain unfolding of Sp in cluster" begins. The tension of the top pair (Sp_1/Sp_2) would remain far smaller than that of the other two pairs, because they would be minimally extended at this deformation angle.

The modular elongation of Sp is a critical component in this model. In both kinds of deformation (equibiaxial and anisotropic), a minor difference in tension within a Sp pair may decide which Sp will unfold first, and in response to that the other Sp may reduce slightly the tension and

length to reach a new equilibrium condition. The tension of one Sp in anisotropic deformation would reach the 30 pN threshold for the first unfolding of Sp when $\lambda_i = 4.24$, which would be larger than the "sustainable" deformation ratios ($\lambda_i \sim 2.5$) as generated in local deformations by micropipette aspiration.[11,12,24] Therefore, it is possible that in a sustainable anisotropic deformation of erythrocyte membrane, none of the Sp may have been unfolded. Modular elongation of Sp, therefore, may be involved in unsustainable erythrocyte deformations, such as in the tether formation or other pathological conditions.[21]

Potential Roles of a Protofilament

The precise angle of the protofilament relative to the lipid bilayer may play a very important role in the mechanics of the network, which may have significant physiological consequences. The angle of the protofilament is an integral part of the network kinetics in response to a mechanical stress, including that of the thermal fluctuation, since three pairs of Sp (top, middle, and bottom pairs) are all connected to a protofilament. As a result, any change of the protofilament angle may affect the tension of each of the 6 Sp, and vice versa. Such interplay between the Sp tensions and the protofilament angles may have significant physiological and pathological consequences. For example, the interplay may transduce the mechanical forces into chemical events in proteins (such as ion channels) that are structurally linked to the network, or quick changes of the yaw angle of protofilaments, dragging along associated transmembrane proteins across the lipid bilayer, may alter the diffusions of oxygen or transport of other molecules across the membrane. Furthermore, large changes of pitch or roll angles may lead to lipid bilayer displacement and/or intrusion of protofilaments or other membrane skeletal proteins through the lipid bilayer and exposure on the cell surface. Such events may trigger immune responses or other recognition events against such mechanically exposed proteins.[27]

CONCLUSION

Using a mesoscale mathematical model for a JC, we are able to predict, for the first time, the magnitude of the tension in each of the 6 Sp and the 3-D orientation of a protofilament in one basic unit of the erythrocyte membrane skeleton. This report predicted these values for the natural state and two experimentally verifiable deformation modes, i.e., equibiaxial and anisotropic deformations. Model predictions are in agreement with experimental FPM data about pitch and yaw angles of the protofilament in these deformation states. The roll angle in response to the Sp extension, on the other hand, is novel and no experimental measurements or model predictions have been made in the past.

During cell deformation, changes of Sp tension and protofilament attitude may transduce mechanical forces into chemical events in the cell and membrane. In that sense, the individual basic unit or the membrane skeleton network as a whole may function as a sensor for different types and ranges of deformation and/or as a controller for physiological responses.

Different conditions such as alterations in the length of the actin filaments (e.g., likely in the absence of E-Tmod capping at the pointed end in *E-Tmod* null erythroid cells)[9] or in the number of associated Sp (e.g., in configurations of pentagons or heptagons)[25] can also be simulated using this model. In addition, both regular and nonregular polygonal configurations may be used. Investigations are also underway to find equilibrium conditions in other important physiological and pathological conditions, such as Sp failures, different Sp to SC connectivity, and SC cross-linking in response to various mechanical or chemical conditions.

This mesoscale model opens a new window to incorporate certain molecular features of JC and, at the same time, takes the advantages of the nonlinear stiffness characterization of the Sp. The dynamic motion and the steady states of JC in response to the mechanical deformation may be the underlying mechanisms in a number of physiological and pathophysiological events in erythrocytes. The ability to understand and predict the nanomechanics at the molecular level may also lay the foundation for designing artificial network structures in biomedical applications and material science.

APPENDIX

Erythrocyte Membrane Structure

The human membrane skeletal network consists of approximately 33,000 basic repeating units. Each basic repeating unit is defined as a small "spoked" but edge-free hexagon formed by a JC with six long Sp radiating from a central short actin protofilament and up to six SC.[38] While one JC is associated with 6 Sp at their proximal (tail) ends, each SC is associated with a Sp near its distal (head) end. The radius of a "spoked" basic unit may depend on the degree of extension of the 6 Sp, which may be as long as $\sim$100 nm in erythrocytes undergoing hypotonic lysis. These repeating units connect with each other through the head-to-head association of Sp from two neighboring units [Fig. A1(b)].

Junctional Complex (JC)

Each JC consists of an actin protofilament of length 35.75 nm, whose twelve G actin subunits are arranged as two right-handed strands intertwined with each other; two coiled-coil of TM of length 33–35 nm, each positioned in the opposite grooves of the protofilament; a globular E-Tmod of about 4 nm in diameter, which caps the pointed

end of the protofilament; and 6 Sp of about 100 nm long, each may be suspended, through a SC, to the lipid bilayer (Fig. A1).[38]

Actin Protofilament

In this numerical model, we use 35.75 nm for an actin filament of 12 G actin[4] and 37 nm for the reinforced protofilament,[33] which contains E-Tmod and/or other associated proteins. Since 35.75 nm is approximately 100 times smaller than the persistence length of the actin filament,[20] the protofilament is considered as a solid rigid cylinder. Since the helical actin filament has an alternating wider diameter of about 9 nm and a narrower diameter of about 7 nm,[4] and each α or β spectrin monomer has a radius of approximately 2 nm filling in the cleft in the protofilament.[1,38] Nine nm is used for the diameter of the rigid body cylinder.

Sp Attachment Site on Protofilament

A 3-D model of JC has been proposed[38] and the coordinates of attachment sites of three Sp pairs on the protofilament are utilized in this mathematical model (Table A1 and Fig. A2). Specifically, the β spectrin attachment sites are positioned at G actin 1b, 2a, 3b, 4a, 5b, and 6a along

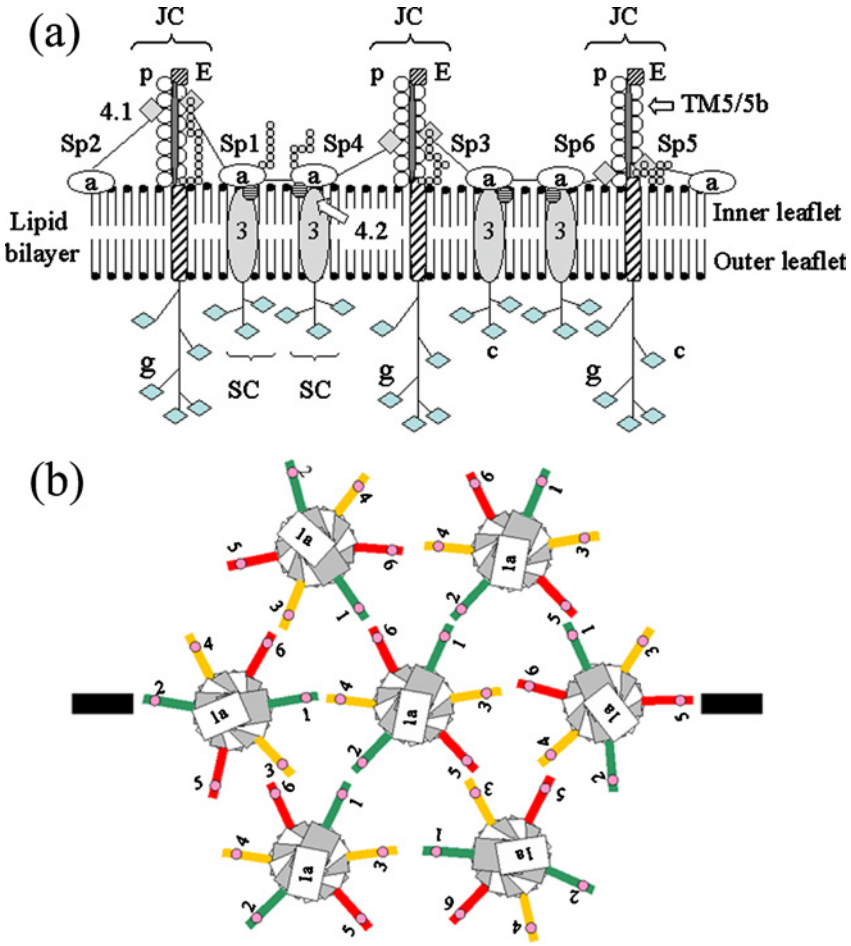

Fig A1. A schematic drawing of the erythrocyte membrane. (a) A cross section showing the spatial relationship among the lipid bilayer, transmembrane proteins, the protofilament, Sp, and other associated proteins. One pair of Sp (i.e., $Sp_{1/2}$, $Sp_{3/4}$, or $Sp_{5/6}$) is shown for each protofilament. *3*, band 3; *4.1*, protein 4.1R; *4.2*, protein 4.2; *a*, ankyrin; *c*, carbohydrate moieties in glycoproteins; *E*, erythrocyte tropomodulin; *g*, glycophorin C; *JC*, junctional complex; *p*, protofilament; *SC*, suspension complex; *Sp*, $\alpha\beta$ spectrin dimer; *TM*, tropomyosin. The cytoplasmic domain of glycophorin C is shown to be associated with protein 4.1R. The cytoplasmic domain of band 3 is also shown between the center and left JC. The dimensions of molecules are not to scale, the helical feature of protofilaments is not shown, and only one glycophorin per JC is shown. Although protofilaments are drawn as perpendicular to the lipid bilayer for clarity, their θ angles are not specified, which are the main subjects of this investigation. (b) The top view of six basic hexagonal units, surrounding a center one, forming a large "spoked" hexagon in the membrane skeletal network.[38] The head-to-head interaction of Sp forms spectrin tetramer *between* adjacent units. The bars on each side indicate the plane of cross-section represented in (a). For clarity, G actin 1, but not E-Tmod, is shown at the pointed end of the protofilament.

Table A1. Coordinates of Sp and SC attachment sites (see Fig. A2).

Sp on the protofilament (nm) in $\{x_b, y_b, z_b\}$ reference frame	SC in the lipid bilayer (nm) in $\{x_a, y_a, z_a\}$ reference frame	
	Natural state $\lambda = 1$	Equibiaxial extension $\lambda = 2.67$
$m_1^b = (0, 4.50, 12.38)$	$h_1^r = (0, 30, 0)$	$h_1^e = (0, 80, 0)$
$m_2^b = (-1.08, -4.37, 9.63)$	$h_2^r = (0, -30, 0)$	$h_2^e = (0, -80, 0)$
$m_3^b = (3.70, 2.56, 1.38)$	$h_3^r = (26, 15, 0)$	$h_3^e = (69, 40, 0)$
$m_4^b = (-4.21, -1.60, -1.38)$	$h_4^r = (-26, -15, 0)$	$h_4^e = (-69, -40, 0)$
$m_5^b = (4.21, -1.60, -9.63)$	$h_5^r = (26, -15, 0)$	$h_5^e = (69, -40, 0)$
$m_6^b = (-3.70, 2.56, -12.38)$	$h_6^r = (-26, 15, 0)$	$h_6^e = (-69, 40, 0)$

the protofilament.[38] The axial stagger of 2.75 nm and a dihedral angle of 166.2° per G actin (e.g., between 1a and 1b) are used to position Sp on the long axis of a protofilament.

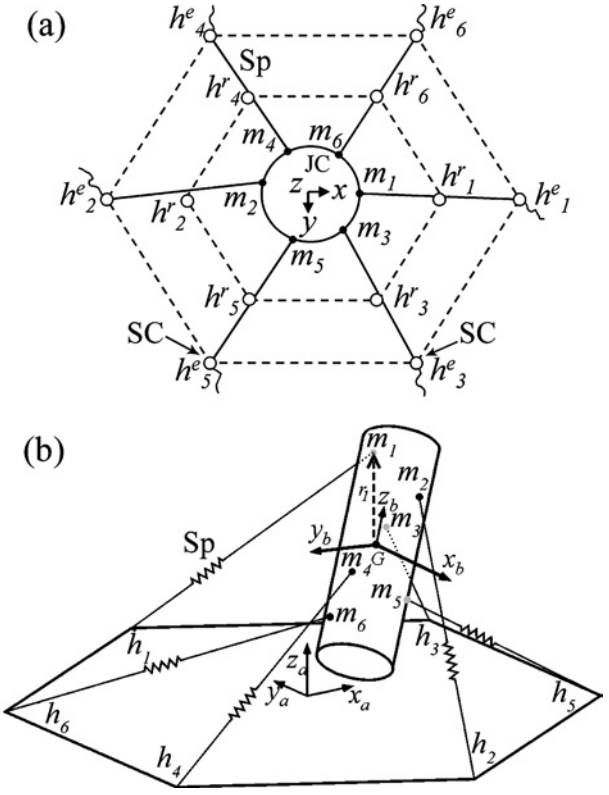

Fig A2. Overall geometry and notations of a basic repeating unit. (a) The top views in the natural ($\lambda = 1$) and an equibiaxial extension state ($\lambda = 2.67$) are presented as inner and outer small hexagons, respectively. For clarity only protofilament, Sp, and SC are shown. The short relaxed line of Sp beyond SC (at $\lambda = 2.67$) is the portion between the ankyrin binding site and the head. The dash lines between SC indicate that they are not connected physically. The drawing is not to scale. (b) 3-D view of a solid rigid body representing the protofilament. Both the Sp attachment sites on the protofilament (m_i), and that of SC in the lipid bilayer (h_i) are shown.

Suspension Complex (SC)

This model considers SC to be anchored to the lipid bilayer, forming the vertices of a hexagon surrounding the protofilament, where the 6 Sp are attached. In reality, the SC are not fixed in the lipid bilayer but rather floating in it, and Sp is not ending at SC but rather extending its head 20 nm or less to connect with the counterpart in the neighboring unit (Figs. A1 and A2). The lipid bilayer of 5 nm thick consists of an outer and inner leaflet [Fig. A1(a)].

The SC provides the main attachment sites for the membrane skeleton to the lipid bilayer. The number of ankryin per ghost is ~120,000, and that for β-spectrin is ~240,000.[16] Therefore, on average, there may be one SC per tetramer and in a random fashion. As the first attempt to mathematically model the basic unit of the membrane skeleton, we chose to have all six sites on the 6 Sp dimers occupied by SC, so that the modified contour length of Sp in a regular hexagon is uniform. In reality 6 SC may only occupy 3 Sp in one basic unit and another 3 Sp which may be 40 nm further away from the JC in a random fashion.

Contact between Protofilament and Lipid Bilayer (K_m)

Within a single unit of erythrocyte membrane skeleton, a vertical stiffness (K_m) is assumed at the contact point between the protofilament and the lipid bilayer. The molecular mechanism providing this mechanical character is not specified. It may include the compression and bending moduli of the lipid bilayer and/or the retention force provided by glycophorin C in the lipid bilayer through associated protein 4.1.

Model Geometry

Figure A2(b) displays the overall geometry of the basic hexagonal unit. The protofilament is represented as a rigid cylinder of 9 nm in diameter and 37 nm in height. It is attached to the erythrocyte membrane lipid bilayer by a network of 6 Sp represented as nonlinear springs. The Sp are attached to the lipid bilayer at locations denoted h_i ($i = 1$–6). These anchorage points describe the locations

of the SC. Table A1 gives the coordinates of the SC in the plane of the lipid bilayer, both in the natural (h_i^r) and an equibiaxial extension (h_i^e) states mentioned in previous sections (Fig. A2). These coordinates are expressed in the reference frame $\{x_a, y_a, z_a\}$, which is fixed to the lipid bilayer at the center of the hexagon. Also shown in Fig. A2(b) are the Sp attachment sites on the protofilament (m_i) corresponding to the configurations discussed earlier. The attachment sites on the protofilament (cylinder) are expressed in the moving reference frame of the cylinder $\{x_b, y_b, z_b\}$, which is fixed to the geometric center of the protofilament. In upcoming mathematical developments, quantities expressed in the lipid bilayer coordinate system $\{x_a, y_a, z_a\}$ and in the protofilament coordinate system $\{x_b, y_b, z_b\}$ are denoted by subscript "a" and "b," respectively.

Modified Contour Length (L_c') of Sp

In this model, Sp acts as a nonlinear spring. The original WLC model of Sp was based on force spectroscopy,[31] which used a full contour length (L_c) of 163.4 nm, and the force–extension curve was based on the force acting at the very ends of Sp. In our model (Fig. A3), the force is applied between the actin binding site (at the N-terminus and the ankyrin binding site on β spectrin at the 15th domain of β spectrin).[2] Since a β spectrin has a total of 17 domains, the force–extension curve of Sp uses a modified contour length (L_c') of 144.2 nm, corresponding to 15/17 of the original L_c.

Tension in Sp

The Sp force–extension curve is obtained using a modified contour length L_c' of 144.2 nm and an average unfolding peak force threshold of 30 pN (Fig. A3).[31] The nonlinear Sp force–extension curve using a WLC model is described by the equation:[5]

$$F(x) = \frac{K_b T}{p}\left(\frac{1}{4(1-(x/L_c)^2} - \frac{1}{4} + \frac{x}{L_c}\right) \qquad \text{(A.1)}$$

In Eq. (A.1), $K_b = 1.3807 \times 10^{-23}, J/K$ is the Boltzmann constant, $p = 0.8$ nm is the persistent length of Sp,[31] T is the temperature, and x is the actual (effective) length between anchorage points (between h_i and m_i in Fig. A2(a), and the horizontal axis in Fig. A3) for each Sp. Each curve in Fig. A3 reaching 30 pN corresponds to Eq. (A.1) with increasing values of L_c' [Fig. 3(b)]. The sequential unfolding of spectrin domains leads to a pronounced saw tooth pattern. At the peak force the weakest of the folded spectrin domains in the chain unfolds (see L_{spuf} in Table A2) in an all-or-none event, adding an additional stretch of unraveled polypeptide to the chain. Hence, the absolute value of the peak force marks the unfolding force of a domain, and the spacing to the following peak reflects the gain in length during a transition from the folded configuration to the fully unraveled polypeptide strand and corresponds to the 106 amino acid residues folded in a spectrin domain.[31]

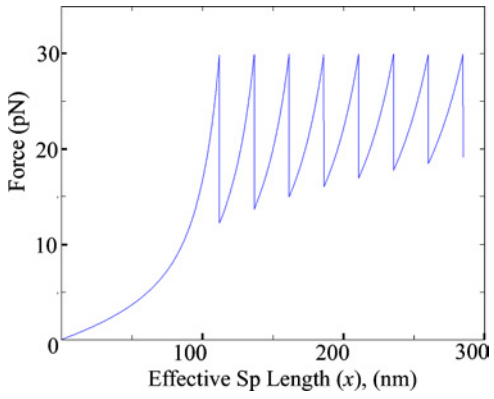

Fig A3. Modified force–extension curve of Sp in WLC model. The Sp force was calculated using the adjusted contour length L_c' of 144.2 nm. The discontinuities in the curve correspond to successive unfolding of spectrin domains. The peak force, 30 pN, of the original curve is used for the unfolding of a domain.[31]

Dynamic Equations of Motion

Whenever the protofilament is in an out-of-equilibrium position, it will move under the action of the forces acting on it (i.e., the 6 Sp plus a possible contact point with the membrane). It will move toward a stable equilibrium position in which the resultant force and torque acting on the protofilament are zero. Although the initial goal of this study was to find the equilibrium position, and not the transient behavior described by the dynamics (i.e., the motion of the protofilament before it reaches equilibrium) of the protofilament, the numerical integration of the equations of motion described in a subsequent section under "*Numerical integration*" constitutes an efficient method to converge to the sought static equilibrium (i.e., method of the dynamic relaxation). This approach turned out to be numerically more efficient than solving the static equilibrium equations iteratively.

The protofilament motion is described using the equations of motion of a rigid body:[32]

$$\text{Translation}: \frac{dP(t)}{dt} = M\frac{dv_G(t)}{dt} = F(t) \qquad \text{(A.2)}$$

$$\text{Rotation}: \frac{dL(t)}{dt} = \frac{d}{dt}[I\omega(t)] = \tau(t) \qquad \text{(A.3)}$$

In these equations (refer to Fig. A4 for notations), P is the linear momentum of the protofilament, L is its angular momentum, M and I are respectively the mass and inertia

Table A2. Input parameters used in the mathematical simulation.

Geometry constraints	Protofilament radius (nm)	4.5
	Protofilament height (nm)	37
	Coordinates of β spectrin binding site on the protofilament (nm)	See m_i^b in Table A1
	Coordinates of SC in equibiaxial extension state (nm)	See h_i^e in Table A1
Membrane mechanical properties	Membrane vertical stiffness K_m(pN/nm)	87.5
	Membrane damping coefficient (pN s/nm)	2
WLC model parameterization [Eq. (A.1) and Fig. A3]	Modified Sp contour length L'_c (nm).	144.2
	Length increments ΔL_c of L'_c after each spectrin domain unfolding (nm)	31.7
	Spectrin unfold threshold L_{spuf} (nm) (adjusted to 30 pN for each spectrin domain unfolding)	[112, 137, 162, 186, 211, 236, 260, 285]
	Persistence length p (nm)	0.8
	(T) temperature (°K)	310
Computational parameters	(dt) time step (s)	0.01
	(t_{fin}) total finite time of simulation (s)	40
	(C_{trans}) damping coefficient for translation (1/s)	2
	(C_{rot}) damping coefficient for rotation (1/s)	0.5
	Initial configuration.	$\psi = 0$, $\theta = 30$, $\phi = -90$ $X_G^a = 0$; $Y_G^a = 0$; $Z_G^a = 0$

tensor (a 3×3 matrix) of the protofilament, $F = \sum_{i=1}^{7} F_i$ is the resultant force applied to the protofilament by the 6 Sp plus the contact point on the membrane, $\tau = \sum_{i=1}^{7} r_i \times F_i$ ("$\times$" denotes the cross-product of two vectors) is the resultant torque produced by those forces around the protofilament mass center (geometric center) G, and $v_G(t)$ and $\omega(t)$ are respectively the translational and angular velocities of the protofilament. The vector of the force F_i (expressed in the inertial referential) in each of the 6 Sp is obtained by projecting its absolute value (Eq. A.1) onto the direction of the Sp:

$$F_i^a = f_i \underbrace{\frac{h_i^a - \left(x_G^a + T m_i^b\right)}{||h_i^a - (x_G^a + T m_i^b)||}}_{l_i} \tag{A.4}$$

where f_i is the tension in Sp_i given by substituting $x = l_i$ in Eq. (A.1). When contact occurs between the protofilament and the membrane, it produces a vertical force F_7 at the contact point:

$$F_7 = -K_m Z_7 \tag{A.5}$$

where K_m is a linear spring representing the erythrocyte membrane vertical stiffness, and Z_7 is the length of the spring.

Equations (A.2) and (A.3) are expressed in the inertial coordinates system $\{x_a, y_a, z_a\}$, so should be $I(t)$. It is obtained from I_0 (the constant, body-fixed inertia tensor) according to

$$I^a(t) = T I_0 T^T \tag{A.6}$$

where T is the 3×3 rotation matrix describing the orientation of the moving referential $\{x_b, y_b, z_b\}$ with respect to the inertial referential $\{x_a, y_a, z_a\}$ [the derivation of T will be given in Eq. (A.12)]. Note that the values of M and I_0 do not affect the final static equilibrium of the system and can be arbitrarily chosen. In the example treated (Fig. A5), M and I_0 are selected to yield a numerically well-conditioned system (i.e. the various translation and rotation motions occur with comparable timescales).

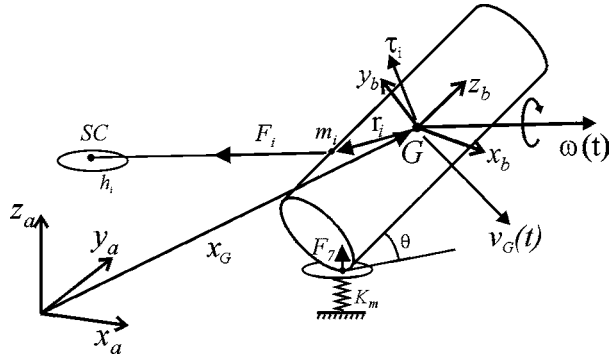

Fig A4. The rigid body model showing the quantities involved in the protofilament dynamic equations (A.2) and (A.3). Only 1 Sp, which is attached to the protofilament and suspended by 1 SC, is represented.

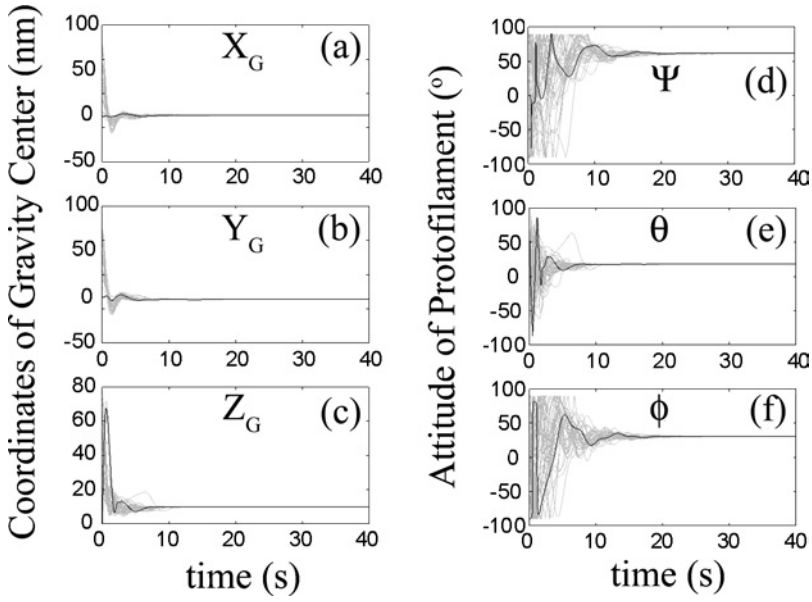

Fig A5. Evolution of protofilament attitude during 40 s of dynamic simulation (equibiaxial deformation). Left panel (a, b, c) shows the position of the geometric center of the protofilament in $\{X_G^a, Y_G^a, Z_G^a\}$ coordinates. Right panel (d, e, f) shows the roll (ψ), pitch (θ), and yaw (ϕ) angles used to describe protofilament orientation. Black lines correspond to the evolution of the protofilament whose initial configuration is given in Table A2, and gray lines correspond to that of 40 other, randomly selected initial configurations (with other parameters unchanged).

Numerical Integration

The dynamic motion of the protofilament is described using a state vector, which contains position and velocity information (for both translation and rotation) of the protofilament:

$$Y(t) = \begin{pmatrix} x_G(t) \\ q(t) \\ P(t) \\ L(t) \end{pmatrix} \tag{A.7}$$

In Eq. (A.7), x_G is the protofilament's center of mass position (in inertial coordinates) and q is a four-element vector (quaternion) describing the rotation of the protofilament (the use of quaternions for describing 3-D rotation of a rigid body is explained at the end of this section). Throughout the simulation, the state vector is updated at every time step Δt, according to:

$$Y(t + \Delta t) = Y(t) + \frac{dY}{dt}(t)\Delta t \tag{A.8}$$

This constitutes a simple (yet sufficient for this model) solver for the system of Ordinary Differential Equations (A.2)–(A.3).

Using Eqs. (A.2) and (A.3) for the derivative of P and L, respectively, and Eq. (A.10) for the derivative of q[34], and after adding damping terms in the translation and rotation equations, the state derivative dY/dt appearing in Eq. (A.8) writes:

$$\frac{dY(T)}{dt} = \frac{d}{dt}\begin{pmatrix} x_G(t) \\ q(t) \\ P(t) \\ L(t) \end{pmatrix} = \begin{pmatrix} v_G(t) \\ \frac{1}{2}[0, \omega(t)] \otimes q(t) \\ F(t) - c_t P(t) \\ \tau(t) - c_r L(t) \end{pmatrix} \tag{A.9}$$

where $\otimes$ stands for the quaternion multiplication operator defined by equation (A.11). At each time step, Eq. (A.9) is used to compute the state derivative from the known state vector $Y(t)$, and in turn, the state vector at the next time step is obtained from Eq. (A.8).

Quaternion Representation of a Rigid Body's Orientation in Space

There are many ways to represent 3-D rotations. It requires at least the definition of three angles like the commonly used Euler's angles, or the roll-pitch-yaw angles used in aeronautics. Although such descriptions have a clear geometric meaning, using them to write the dynamic equations of a rigid body leads to heavy trigonometric expressions. On the other hand, direction cosine matrices are numerically easy to use, but they possess a high degree of redundancy (nine coefficients to describe three angles), so a unitary constraint on the matrix must be added, $T^T T = I$.

As a direction cosine matrix $T(t)$ is updated throughout the simulation, numerical drift will be inevitably encountered. This error in T coefficients will add up progressively, so that T will no longer be precisely a rotation matrix.

Graphically, applying T to the moving body would cause a skewing effect. Because of this, a unit quaternion representation of 3-D rotations is chosen.[34] A rotation of magnitude θ around the axis defined by a unitary vector u is represented by the four-element vector:

$$q = \left[\underbrace{\cos(\theta/2)}_{s}, \underbrace{u_x \sin(\theta/2), u_y \sin(\theta/2), u_z \sin(\theta/2)}_{v}\right] = [s, v] \tag{A.10}$$

The "quaternion product," used for the derivation of dq/dt in Eq. (A.9), is defined by

$$\begin{aligned} q_1 \otimes q_2 &= [s_1, v_1] \otimes [s_2, v_2] \\ &= [s_1 s_2 - v_1 \cdot v_2, s_1 v_2 + s_2 v_1 + v_1 \times v_2] \end{aligned} \tag{A.11}$$

where a "·" denotes the scalar product of two three-element vectors and "×" their cross-product.

The unit quaternion representation provides an effective way of integrating the dynamic equation of the protofilament orientation. It is still necessary to compute the corresponding rotation matrix $T(t)$ at every time step to easily locate any point attached to the protofilament cylinder. T is computed from q as follows:

$$\begin{aligned} q &= [s, \upsilon_x, \upsilon_y, \upsilon_z] \Leftrightarrow T \\ &= \begin{pmatrix} 1 - 2\upsilon_y^2 - 2\upsilon_z^2 & 2\upsilon_x\upsilon_y - 2s\upsilon_z & 2\upsilon_x\upsilon_z + 2s\upsilon_y \\ 2\upsilon_x\upsilon_y + 2s\upsilon_z & 1 - 2\upsilon_x^2 - 2\upsilon_z^2 & 2\upsilon_y\upsilon_z - 2s\upsilon_x \\ 2\upsilon_x\upsilon_z - 2s\upsilon_y & 2\upsilon_y\upsilon_{z+} + 2s\upsilon_x & 1 - 2\upsilon_x^2 - 2\upsilon_y^2 \end{pmatrix} \end{aligned} \tag{A.12}$$

The converse relation is

$$\begin{cases} s = 1/2\sqrt{(1 + \text{trace}(T)} \\ \upsilon x = \frac{0.5(r32 - r23)}{\sqrt{1+\text{trace}(T)}} \\ \upsilon y = \frac{0.5(r13 - r31)}{\sqrt{1+\text{trace}(T)}} \\ \upsilon z = \frac{0.5(r21 - r12)}{\sqrt{1+\text{trace}(T)}} \end{cases} \tag{A.13}$$

where r_{ij} represents the ith row jth column element of T.

Implementation of Numerical Solution

Application software was developed using MATLAB (Release 13, version 6.5, MathWorks Inc., Natick, MA). The dynamic relaxation method was used to solve the 6 degree-of-freedom model. Although a quaternion representation (the four Euler parameters) is used to calculate the protofilament orientation during the numerical integration of the dynamic equations, it does not have a clear geometric meaning suitable for physical interpretation. Instead, in the present simulation results, the orientation of the protofilament is described using a set of three angles $\{\psi, \theta, \text{and } \phi\}$, analog to the "roll pitch yaw" angles used in aeronautics [Fig. 1(b)]. Angle ψ(roll) describes a rotation of the protofilament around its longitudinal axis x_a (counted positive when y_a rotates toward z_a), angle θ (pitch) describes the protofilament angle to the horizontal plane (rotation around axis y_a, counted positive when the pointed end of the protofilament moves from x_a toward z_a), and angle ϕ (yaw) describes the rotation of the protofilament around the axis z_a (counted positive when x_a rotates toward y_a). The displacement of the contact point of the protofilament in respect to the lipid bilayer is denoted P_{intr} [$-Z_7$ in Eq. (A.5)].

Evolution of protofilament attitude during maximal equibiaxial deformation is presented in Fig. A.5. The black line shows the evolution of the protofilament position and orientation during a 40 sec simulation time. It can be observed from the solid line that, after a transient motion due to the out-of-equilibrium initial configuration (Table A2, bottom row), the protofilament stabilizes around its static equilibrium. The results of the simulation corresponding to the final static equilibrium (at $t = 40$ s) are given in Table A3. An additional 40 simulations were run with randomly selected initial configurations. Each of the three angular coordinates was selected in a range of 360°, and each of the three coordinates of the geometric center was selected in a range of 80 nm. The gray curves in Fig. A.5 show the evolution of X_G^a, Y_G^a, Z_G^a and θ, ϕ, ψ for the 40 additional random initial configurations. All simulations clearly converge to the same final equilibrium state.

Model Limitations

The calculations of the protofilament attitude and Sp tension depend on several key model assumptions, which

Table A3. The static equilibrium of the protofilament and 6 Sp at $\lambda = 2.67$

Protofilament orientation [ψ, θ, ϕ] (°)	[62, 18, 30]
Protofilament geometric center [X_G^a, Y_G^a, Z_G^a] (nm)	[1.1, −2.4, 9.9]
Final length $\{l_i, i = 1...6\}$ of each Sp cable (nm)	[74, 81, 78, 78, 80, 74]
Final tension $\{f_i, i = 1...6\}$ in each Sp cable (pN)	[7, 9, 8, 8, 8, 7]
Final normal force $\{n_i, i = 1...6\}$ in each SC (pN)	[1.1, 1.7, 0.6, 1.4, 0.4, 0.8]
Resultant force at protofilament [R_x, R_y, R_z] (pN)	[0, 0, 6]

Note. Values are rounded to integral values, except for the normal force and the coordinates of geometric center.

were chosen as close as possible (but may not be identical) to the physiological conditions. These include the assumption as rigid body for a protofilament, the free rotation and translation for a protofilament, the 3-D attachment mode of 6 Sp to a protofilament, the Sp-protofilament attachment as a mechanical ball-joint, the WLC model for the force–extension of Sp, the regular hexagonal geometry for 6 SC, the fixed 2-D final positions for SC, the K_{m}, the order of connections between Sp and SC, and the damping coefficient values. Some of these assumptions are further discussed below.

(1) A simple mechanical ball-joint was used to model the Sp-protofilament interaction, even though a split α and β spectrin were proposed to wrap around a protofilament.[38] In the wrap around model, the extension of α and/or β spectrin around the protofilament may provide a mechanism to minimize the torque applied to the protofilament during deformation, affecting roll and possibly yaw angles. Since Sp is highly flexible and its length is an order of magnitude larger than the diameter of the protofilament, the specific character of the boundary condition (attachment) at this level of modeling, may not be of much significance.

(2) The only available WLC for the force–extension of Sp is based on AFM force spectroscopy of monomeric spectrin (not dimeric Sp) pretreated by high pH.[31] According to this relationship, all Sp were in tension even at natural state [Fig. A.3 and Eq. (A.1)], but in reality Sp may not be in tension until it reaches a critical length–resting length, which is unknown to us (Fig. 1a). Furthermore, the influence of strong lateral associations of antiparallel spectrin heterodimers, which facilitate simultaneous unfolding of spectrin repeats,[22] has not been taken into consideration. Simultaneous unfolding may require higher force (perhaps ~40 pN) as compared to a single domain unfolding (~25–35 pN).[31] In that case, even higher deformation ratios would be needed to begin unfolding Sp *in vivo* in both equibiaxial and anisotropic deformations. No mathematical models for native Sp without high pH pre-treatment thus far are available.

(3) The simulation reported here is based on one connectivity mode between Sp and SC (i.e., Sp_i connects to SC_i, $i = 1$–6). This model also does not consider the connectivity beyond one basic unit with other units. Associations among repeating units may modify the coordinates of SC, tension of Sp and attitude of protofilament. Thus, the specified extensions may not correlate directly with macroscopic deformation of the cell. A global minimization for all of the skeletal elements will be performed in order to see how macroscopic membrane deformations result in local molecular extension; more complex 3-D models consisting of multiple units are currently being developed.

And (4) as a first attempt, K_m was introduced as the vertical stiffness of the erythrocyte membrane for the contact between a protofilament and the lipid bilayer, and modeled as a simple linear spring. The model predictions for the attitude of protofilaments are essentially independent of K_m, except for the pitch angle when K_m values are between 0 and ~10 pN/nm (Fig. 2). Our intention is to develop a multi-unit model with lateral movement freedom for SC in the immediate future and incorporate other improvements, such as a positive value for Sp resting length (currently = 0). The preliminary results using a multi-unit model of the network have shown that the compensatory effect of neighboring units may provide the boundary conditions necessary for the protofilament of each unit to be tangent to the lipid bilayer, even in the absence of a vertical stiffness. This interesting finding will be further investigated.

Our model predicts the final deterministic position of a protofilament in response to a deterministic extension. Thermal fluctuation of a flexible protein network may be significant in the mechanics of a JC[23] and the degree of significance will depend on its magnitude (and bandwidth) exerted on the network relative to that induced by the extensions produced. The mechanical noise, which is a function of the system entropy, can be added to parameters of this model including the force–extension curve of Sp, thus allowing molecules to sample multiple orientations over short time scales.

The purpose of this paper is to introduce this new idealized model for the physical problem, i.e., to mathematically simulate the mechanics of a newly modeled JC[38] in response to single unit deformations. In general, there are two methods to find the equilibria: dynamic relaxation and solving the equilibrium conditions algebraically. We have derived the algebraic conditions for the equilibria, but chose to use the dynamic relaxation method because the nonlinear algebraic conditions are not convex problems to solve, and the iterative solutions are probably not more accurate than the dynamic relaxation method we used. Besides, Sp was modeled as a nonlinear spring with modular elongation (see force–extension curve in Fig. A.3). It would be difficult to solve the nonlinear algebraic model using the unfolding extensions of Sp, particularly due to its discontinuity. In the dynamic relaxation method, the actual values of body mass, inertia and damping coefficients affect the dynamic behavior of the system but may not the final equilibrium state, which is the subject of this paper. We do not have physiological values of the damping coefficients; they were chosen to produce a rapid convergence to the final equilibrium state.

ACKNOWLEDGMENTS

This work was supported by NIH Research Grant PO1HL-43026-6 from the National Heart, Lung, and Blood Institute (Project 2, LAS). Frederic Bossens was supported by a postdoctoral fellowship from Skelton's Structural Systems and Control Lab at UCSD, and from the Belgian American Educational Foundation. Carlos Vera was supported by a predoctoral fellowship from

UCMEXUS-CONACYT and a postdoctoral fellowship from Sung's Molecular Bioengineering Lab.

REFERENCES

[1] Almqvist, N., L. Backman, and S. Fredriksson. Imaging human erythrocyte spectrin with atomic force microscopy. *Micron* 25:227–232, 1994.

[2] Bennett, V., and A. J. Baines. Spectrin and ankyrin-based pathways: Metazoan inventions for integrating cells into tissues. *Physiol. Rev.* 81:1353–1392, 2001.

[3] Bennett, V., and P. J. Stenbuck. The membrane attachment protein for spectrin is associated with band 3 in human erythrocyte membranes. *Nature* 280:468–473, 1979.

[4] Bremer, A., and U. Aebi. The structure of the F-actin filament and the actin molecule. *Curr. Opin. Cell Biol.* 4:20–26, 1992.

[5] Bustamante, C., J. F. Marko, E. D. Siggia, and S. Smith. Entropic elasticity of lambda-phage DNA. *Science* 265:1599–600, 1994.

[6] Byers, T. J., and D. Branton. Visualization of the protein associations in the erythrocyte membrane skeleton. *Proc. Natl. Acad. Sci. USA* 82:6153–6157, 1985.

[7] Carrion-Vazquez, M., A. F. Oberhauser, T. E. Fisher, P. E. Marszalek, H. Li, and J. M. Fernandez. Mechanical design of proteins studied by single-molecule force spectroscopy and protein engineering. *Prog. Biophys. Mol. Biol.* 74:63–91, 2000.

[8] Chien, S., K.-L. P. Sung, R. Skalak, S. Usami, and A. Tozeren. Theoretical and experimental studies on viscoelastic properties of erythrocyte membrane. *Biophys. J.* 24:463–487, 1978.

[9] Chu, X., J. Chen, M. C. Reedy, C. Vera, K. L. Sung, and L. A. Sung. E-Tmod capping of actin filaments at the slow-growing end is required to establish mouse embryonic circulation. *Am. J. Physiol. Heart. Circ. Physiol.* 284:H1827–H1838, 2003.

[10] Discher, D. E., D. H. Boal, and S. K. Boey. Simulations of the erythrocyte cytoskeleton at large deformation. II. Micropipette aspiration. *Biophys. J.* 75:1584–1597, 1998.

[11] Discher, D. E., and P. Carl. New insights into red cell network structure, elasticity, and spectrin unfolding–a current review. *Cell Mol. Biol. Lett.* 6:593–606, 2001.

[12] Discher, D. E., N. Mohandas, and E. A. Evans. Molecular maps of red cell deformation: Hidden elasticity and in situ connectivity. *Science* 266:1032–1035, 1994.

[13] Evans, E. A. New membrane concept applied to the analysis of fluid shear- and micropipette-deformed red blood cells. *Biophys. J.* 13:941–954, 1973.

[14] Evans, E. A. Minimum energy analysis of membrane deformation applied to pipet aspiration and surface adhesion of red blood cells. *Biophys. J.* 30:265–284, 1980.

[15] Evans, E. A., R. Waugh, and L. Melnik. Elastic area compressibility modulus of red cell membrane. *Biophys. J.* 16:585–595, 1976.

[16] Fowler, V. M. Regulation of actin filament length in erythrocytes and striated muscle. *Curr. Opin. Cell Biol.* 8:86–96, 1996.

[17] Hansen, J. C., R. Skalak, S. Chien, and A. Hoger. An elastic network model based on the structure of the red blood cell membrane skeleton. *Biophys. J.* 70:146–166, 1996.

[18] Hansen, J. C., R. Skalak, S. Chien, and A. Hoger. Influence of network topology on the elasticity of the red blood cell membrane skeleton. *Biophys. J.* 72:2369–2381, 1997.

[19] Harper, S. L., G. E. Begg, and D. W. Speicher. Role of terminal nonhomologous domains in initiation of human red cell spectrin dimerization. *Biochemistry* 40:9935–9943, 2001.

[20] Kas, J., H. Strey, J. X. Tang, D. Finger, R. Ezzell, E. Sackmann, and P. A. Janmey. F-actin, a model polymer for semiflexible chains in dilute, semidilute, and liquid crystalline solutions. *Biophys. J.* 70:609–625, 1996.

[21] Knowles, D. W., L. Tilley, N. Mohandas, and J. A. Chasis. Erythrocyte membrane vesiculation: Model for the molecular mechanism of protein sorting. *Proc. Natl. Acad. Sci. USA* 94:12969–12974, 1997.

[22] Law, R., S. Harper, D. W. Speicher, and D. E. Discher. Influence of lateral association on forced unfolding of antiparallel spectrin heterodimers. *J. Biol. Chem.* 279:16410–16416, 2004.

[23] Lee, J. C., and D. E. Discher. Deformation-enhanced fluctuations in the red cell skeleton with theoretical relations to elasticity, connectivity, and spectrin unfolding. *Biophys. J.* 81:3178–3192, 2001.

[24] Lee, J. C., D. T. Wong, and D. E. Discher. Direct measures of large, anisotropic strains in deformation of the erythrocyte cytoskeleton. *Biophys. J.* 77:853–864, 1999.

[25] Liu, S. C., L. H. Derick, and J. Palek. Visualization of the hexagonal lattice in the erythrocyte membrane skeleton. *J. Cell Biol.* 104:527–536, 1987.

[26] McGough, A. M., and R. Josephs. On the structure of erythrocyte spectrin in partially expanded membrane skeletons. *Proc. Natl. Acad. Sci. USA* 87:5208–5212, 1990.

[27] Onuma, E. K., P. S. Amenta, K. Ramaswamy, J. J. Lin, and K. M. Das. Autoimmunity in ulcerative colitis (UC): A predominant colonic mucosal B cell response against human tropomyosin isoform 5. *Clin. Exp. Immunol.* 121:466–471, 2000.

[28] Picart, C., P. Dalhaimer, and D. E. Discher. Actin protofilament orientation in deformation of the erythrocyte membrane skeleton. *Biophys. J.* 79:2987–3000, 2000.

[29] Picart, C., and D. E. Discher. Actin protofilament orientation at the erythrocyte membrane. *Biophys. J.* 77:865–878, 1999.

[30] Reid, M. E., Y. Takakuwa, J. Conboy, G. Tchernia, and N. Mohandas. Glycophorin C content of human erythrocyte membrane is regulated by protein 4.1. *Blood* 75:2229–2234, 1990.

[31] Rief, M., J. Pascual, M. Saraste, and H. E. Gaub. Single molecule force spectroscopy of spectrin repeats: Low unfolding forces in helix bundles. *J. Mol. Biol.* 286:553–561, 1999.

[32] Riley, W. F., and L. D. Sturges. Engineering Mechanics: Dynamics. New York: Wiley, 1995.

[33] Shen, B. W., R. Josephs, and T. L. Steck. Ultrastructure of the intact skeleton of the human erythrocyte membrane. *J. Cell Biol.* 102:997–1006, 1986.

[34] Shoemake, K. Animating rotation with quaternion curves. *Comp Graph (Proc. SIGGRAPH)* 19:245–254, 1985.

[35] Smith, B. L., T.E. Schaffer, M. Viani, J.B. Thompson, N.A. Frederick, J. Kindt, A. Belcher, G.D. Stucky, D.E. Morse, and P.K. Hansma. Molecular mechanistic origin of the toughness of natural adhesives, fibers and composites. *Nature* 399:761–763, 1999.

[36] Speicher, D. W., and V. T. Marchesi. Erythrocyte spectrin is comprised of many homologous triple helical segments. *Nature* 311:177–180, 1984.

[37] Sung, K.-L. P., G. W. Schmid-Schönbein, R. Skalak, G. B. Schuessler, S. Usami, and S. Chien. Influence of physicochemical factors on rheology of human neutrophils. *Biophys. J.* 39:101–106, 1982.

[38] Sung, L. A., and C. Vera. Protofilament and hexagon: a three-dimensional mechanical model for the junctional complex in the erythrocyte membrane skeleton. *Ann. Biomed. Eng.* 31:1314–1326, 2003.

[39] Tozeren, A., R. Skalak, K. L. Sung, and S. Chien. Viscoelastic behavior of erythrocyte membrane. *Biophys. J.* 39:23–32, 1982.